Supporting Information for Metabolic Cycling without Cell Division Cycling in Respiring Yeast

Nikolai Slavov[1,4], Joanna Macinskas[2], Amy Caudy[3], and David Botstein[2,4]
[1] MIT, Cambridge, MA 02139, USA
[2] Princeton University, Princeton, NJ 08544, USA
[3] University of Toronto, Toronto, Canada
[4] To whom correspondence should be addressed. E-mail: nslavov@alum.mit.edu, botstein@princeton.edu

Abbreviations: CDC - cell division cycle; GR - growth rate; YMC - yeast metabolic cycle; HOC - high oxygen consumption; LOC - low oxygen consumption; EAP - ensemble average over phases;

1 Culture Conditions and Oxygen Consumption

In addition to the culture shown in the paper, we have synchronized multiple independent cultures (Figure S1) in the same media and growth conditions. The medium used in the experiments was identical with the one we used previously to study the growth rate response of phosphate limited cultures growing in ethanol carbon source (1). It contained $[KH_2PO_4] = 20mg/L$ as the only source of phosphorous and $100mM$ ethanol as the only source of carbon and energy. All other essential nutrients have the same concentrations as the ones used by Saldanha et al. (2), Brauer et al. (3, 4). We have demonstrated that in this growth medium the growth of the culture is limited on phosphate and both the final biomass of batch cultures and the steady–state biomass density of continuous cultures depend linearly on the concentration of phosphate (1). The cultures were grown at 30^oC in $500mL$ chemostat vessels (Sixfors; Infors AG, Bottmingen, Switzerland) containing $500mL$ of culture volume, stirred at $400rpm$, and aerated with humidified and filtered air. Chemostat cultures were inoculated, grown and monitored in batch conditions with no influx of fresh media. The oxygen content in the media of all cultures was measured continuously using oxygen electrodes.

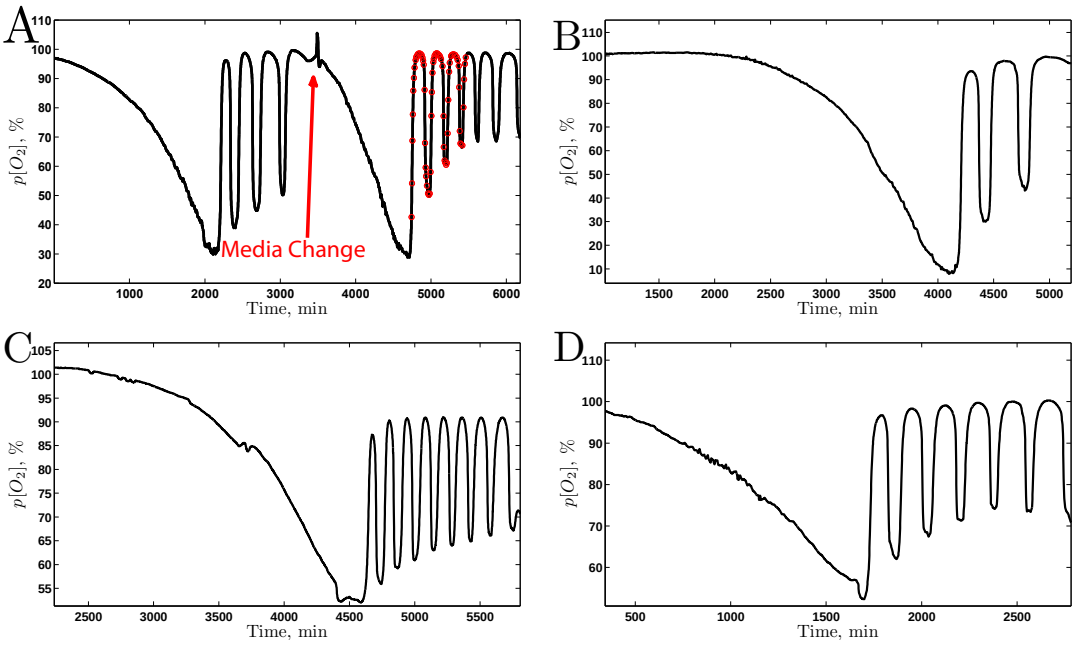

Figure S1. Oxygen Consumption Dissolved oxygen data in 4 independent batch cultures that were metabolically synchronized in phosphate-limited media with ethanol as a sole source of carbon and energy. The conditions are the same as for the culture discussed in the main article.

Since each sample ($2.5ml$) removed 0.5% of the culture, the total cell number in the cultures is reduced (even though the cell density is not affected) by the sampling compared to what it would have been without the sampling. Since we measured both the cell number and the volume of each sample, we can compensate for the removal of cells and calculate what the oxygen consumption would have been without the sampling, Figure S2.

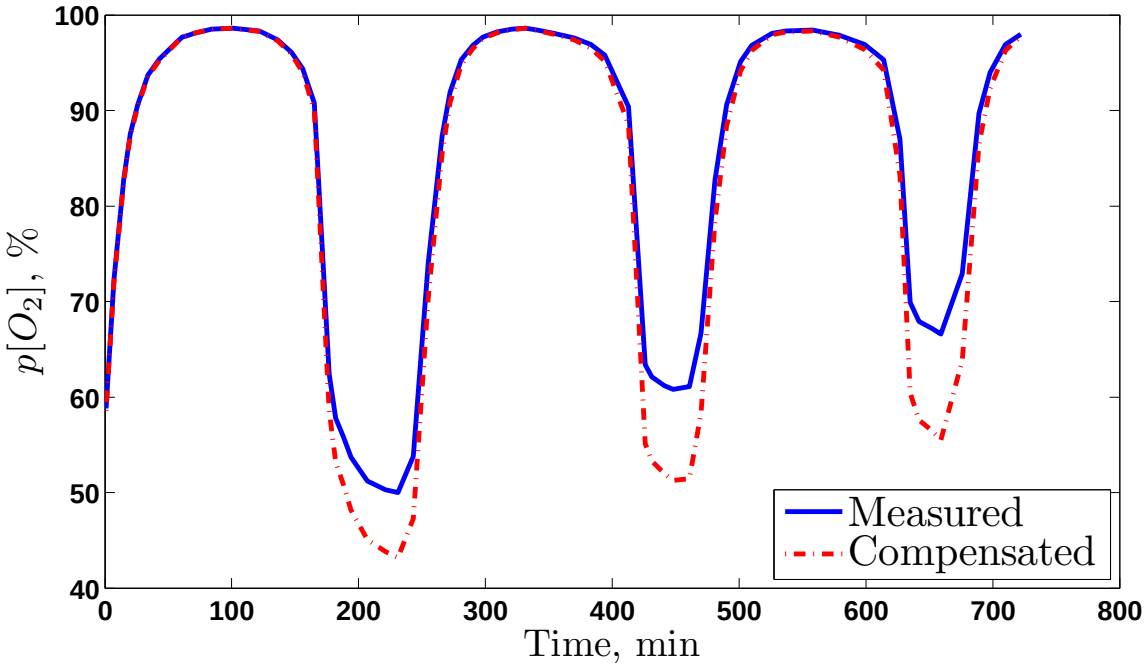

Figure S2. Compensated Oxygen Consumption Oxygen compensated for the decrease in biomass because each sample removed 0.5% of the culture.

1.1 Phases of the Metabolic Cycle Defined by Oxygen Consumption

We measured directly dissolved oxygen in the medium, which tracks very closely the oxygen consumption: Increasing the oxygen consumption of a carbon-source-limited culture by injecting a carbon source results in precipitous drop of the dissolved oxygen within seconds (5). The drop in dissolved oxygen is very fast even when a glucose-limited culture is pulsed with acetate (6). To characterize our metabolically cycling culture, we portioned each metabolic cycle into a phase of low oxygen consumption (LOC) and a phase high oxygen consumption (HOC), Figure S3. Such portioning can be quantified on the basis of the the bimodal distribution of oxygen consumption.

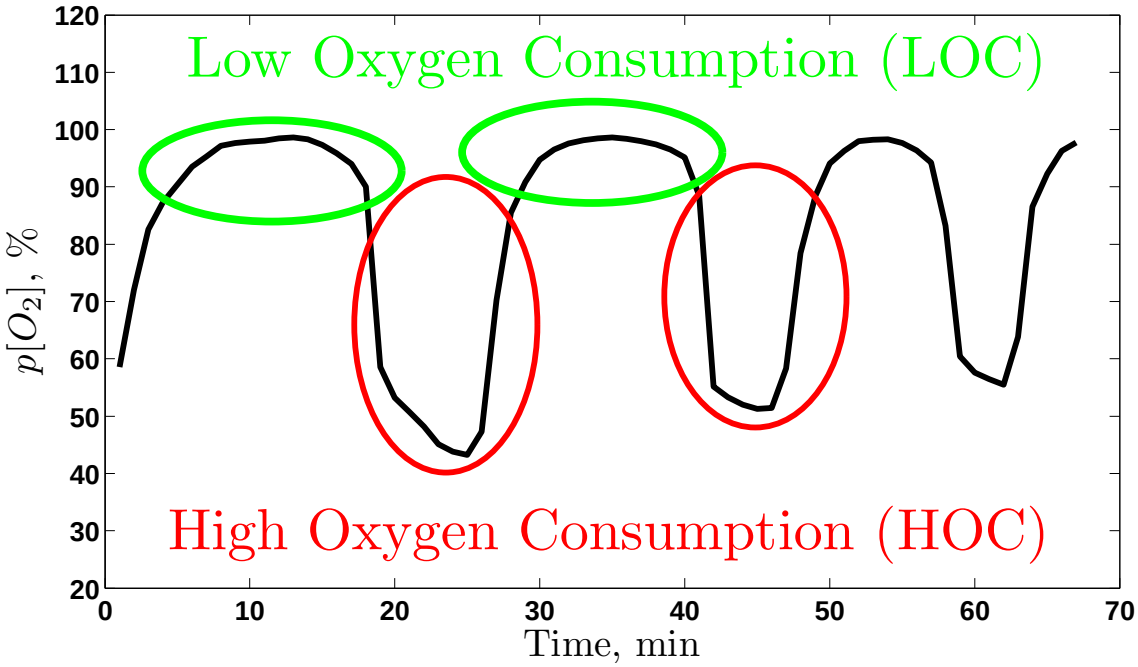

Figure S3. High and Low Oxygen Consumption Phases Each metabolic cycle can be portioned into a phase of low oxygen consumption (LOC) and a phase of high oxygen consumption (HOC)

1.2 Normalization of Oxygen Consumption

The level of dissolved oxygen in the media that we measured depends both on the rate of aeration (volume of air bubbled through the culture per unit time) and on the rate of oxygen consumption by the cells in the culture. Since we are interested only in the rate of oxygen consumption by the culture, we normalized to remove the dependence on the rate of aeration. As a result, the oxygen data in Figures 2, 3 and 4 data reflect the oxygen consumption relative to the maximal consumption of the culture and not relative to the rate of air flow through the media. In particular, we computed normalized dissolved oxygen so that the value ranges from zero during the maximal oxygen consumption to 100 in the absence of cells (as measured in the growth media before inoculation). This transformation was applied based on the steps below:

1. The oxygen consumed by the culture (ζ) is equal to the dissolved oxygen in the absence of cells (before inoculation, which is normalized to 100) minus the oxygen that has not been consumed and is thus in the media: $\zeta = 100-$ Measured_Dissolved_Oxygen;

2. The oxygen consumed by the culture (ζ) was then normalized to ζ_n so that ζ_n varies between 0 (no cells in the culture) and 100 (the maximum measured rate of oxygen consumption): $\zeta_n = \frac{100}{\max(\zeta)}\zeta$

3. Finally, we converted ζ_n back to dissolved oxygen, $p[O_2] = 100 - \zeta_n$

2 Cell Density and Distributions of Cell Sizes

The fraction of budded cells, cell density, cell sizes and ethanol concentration were measured as previously described by Slavov and Botstein (1), Brauer et al. (3, 4). For each time point, $400\mu l$ of culture was sampled in $1.5ml$ eppendorf tube, immediately sonicated and analyzed on a Coulter counter (model Z2; Beckman Coulter, Fullerton, CA) for cell density and cell size distribution. Each sample (corresponding to a time point) was analyzed by the Coulter counter at least in triplicate and the data from all runs averaged.

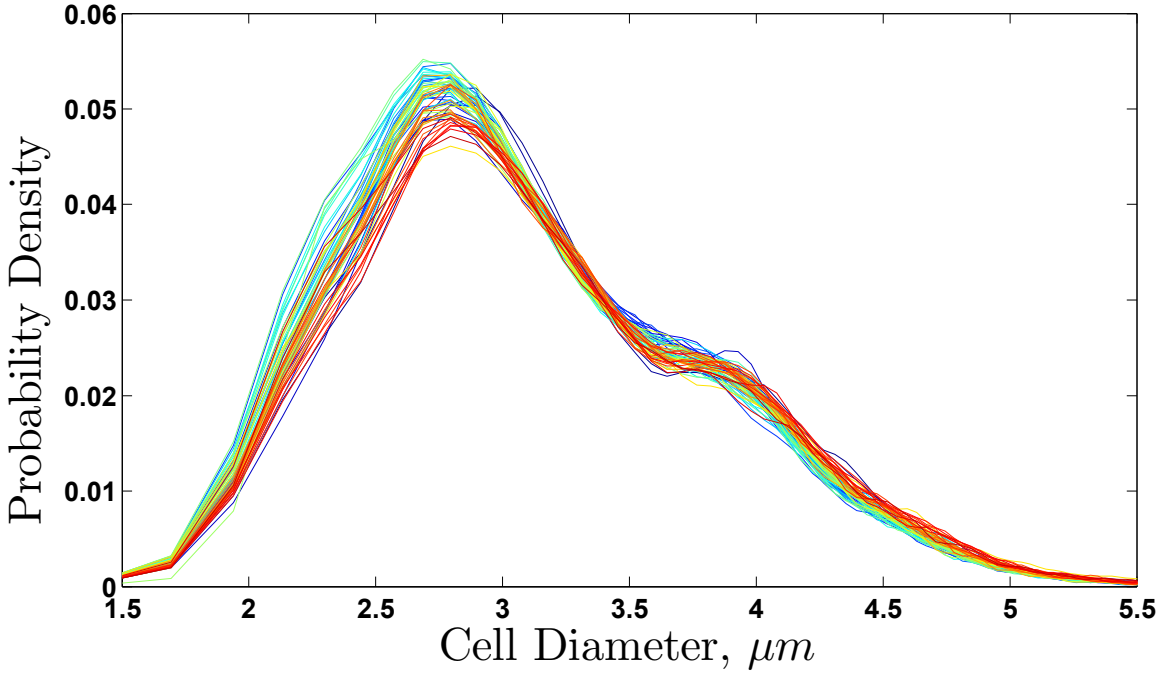

Figure S4. Distributions of Cell Sizes The distributions of cell sizes for the time points from Figure 2 in the paper are rainbow color coded, with blue corresponding to the first time point and red corresponding to the last.

3 Measuring mRNA

To measure mRNA levels, we used *2ml* of the culture sampled at each time point and vacuum filtered the cells followed by immediate freezing in liquid nitrogen and then in a freezer at -80^oC. RNA for microarray analysis was extracted by the acid–phenol–chloroform method. RNA was amplified and labeled using the Agilent low RNA input fluorescent linear amplification kit (P/N 5184-3523; Agilent Technologies, Palo Alto, CA). This method involves initial synthesis of cDNA by using a poly(T) primer attached to a T7 promoter. Labeled cRNA is subsequently synthesized using T7 RNA polymerase and either *Cy3* or *Cy5* UTP. Each *Cy5*-labeled experimental cRNA sample was mixed with the *Cy3*-labeled reference cRNA and hybridized for $17h$ at 65^oC to custom Agilent Yeast oligo microarrays $8 \times 15k$ having 8 microarrays per glass slide. Microarrays were washed, scanned with an Agilent DNA microarray scanner (Agilent Technologies), and the resulting TIF files processed using Agilent Feature Extraction Software version 7.5. Resulting microarray intensity data were submitted to the PUMA Database for archiving.

4 Ordering Genes by Phase of Peak Expression

Among the many possible approaches for finding the phase of peak expression of each gene, we chose correlation analysis for its simplicity. The algorithm that we used has the following steps:

- For each experiment (three cycles), the data for the oxygen consumption and for the i^{th} gene were interpolated at 150 equally spaced time points resulting in two vectors, $\mathbf{o}$ and $\mathbf{g}_i$ for the oxygen and the gene expression respectively, $\mathbf{o} \in \mathbb{R}^{150}$ and $\mathbf{g}_i \in \mathbb{R}^{150}$
- A vector of correlations ($\mathbf{r} \in \mathbb{R}^{40}$) was computed by sliding the two interpolated vectors ($\mathbf{o}$ and $\mathbf{g}_i$) relative to each other, one element at a time for the first 40 elements.
- The index (position) of the largest element of $\mathbf{r}$ was selected to represent the phase (ϕ) of peak expression of the i^{th} gene: $\phi = \arg\max_j \mathbf{r}(j), \quad j = 1 \ldots 40$
- The genes were ordered by sorting the phases ϕ of all genes for which the maximum correlation between $\mathbf{o}$ and $\mathbf{g}_i$ exceeded a threshold.

Since we sought to identify genes with the same phase of peak expression in our batch culture and in the continuous culture (7), we stacked the vectors of oxygen consumption of the two cultures into a single vector $\hat{\mathbf{o}}$, matching the phases of the two cultures. Similarly, the vectors of gene expression for the i^{th} gene were combined into a single vector $\hat{\mathbf{g}}_i$. The correlations were computed by averaging across both datasets, i.e. the correlations between $\hat{\mathbf{o}}$ and $\hat{\mathbf{g}}_i$. The threshold used in Figure 3B was $r_\phi > 0.45$. The threshold used in Figure 4 was $r_\phi > 0.5$. These thresholds correspond to false discovery rates below 5%. There are many algorithms that may improve the outlined approach to estimating the phase of peak expression and phase ordering. This approach is among the simplest possible and it worked very well, see Figure 3B in the article.

5 Amplitudes of YMC Periodic Genes

To compare the metabolic cycling in our batch culture and in the continuous glucose culture (7), we used two metrics to quantify the amplitudes of oscillation for each of the 3000 most periodic genes in both datasets, Figure 3B. Both metrics were applied to the expression vectors, $\log_2$ ratios of the level at each time point relative to the mean for all time points. The first metric is the standard deviation of the expression vectors and the second one the differences between the lowest to the highest expression level. The results (Figure S5) indicate that the distributions for both metrics are very similar for our dataset and for the dataset by Tu et al. (7). The means of the distributions differ by less than 10% and the medians are even closer to each other. Note that the quantification of the amplitude does not depend at all on the normalization, subtraction of the mean expression. In both datasets, hundreds of genes change in expression level more than 10 fold between their lowest and highest expression levels in the metabolic cycle, Figure S5.

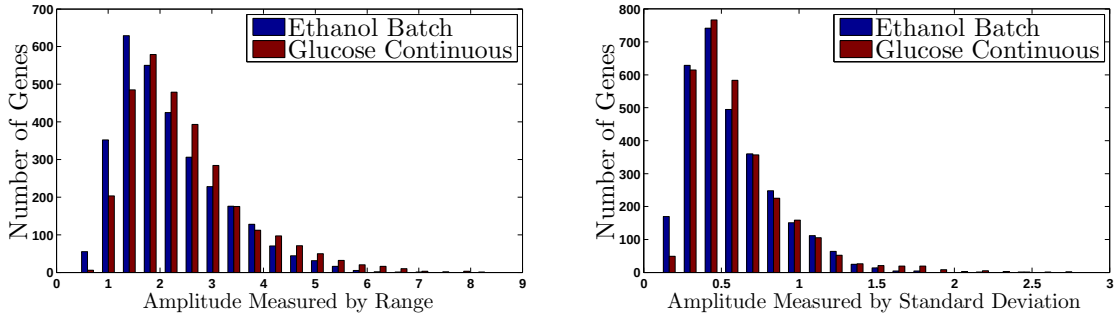

Figure S5. Distributions of the Amplitudes of Oscillation The amplitudes of oscillation of the 3000 most periodic genes from Figure 3B, from our batch culture and from the continuous glucose culture (7), were measured by the standard deviation of the expression vectors or by the change in expression from the lowest to the highest expression level. The results from both metrics are plotted as distributions of amplitudes.

6 Amplitudes for HOC and LOC genes

In our batch culture, genes that peak in LOC generally have higher mean expression levels relative to the reference, a glucose-limited, asynchronous culture growing exponentially at growth rate $\mu = 0.25h^{-1}$. The reverse holds for genes peaking in HOC, Figure 3A. A simple reason for this observation could be that only a fraction of the culture is metabolically cycling and the other fraction of the culture is already arrested in a LOC-like state. This idea is further supported by the observation that the dynamical range (amplitude) of oscillation is larger for the HOC genes (mean variance 0.67) compared to the amplitude for the LOC genes (mean variance 0.35), Figure 3A; when the metabolically cycling fraction of the cells goes through LOC phase the *fractional/relative* increase in the levels of LOC genes would be smaller if the arrested fraction is constantly expressing LOC genes at high levels. Conversely, if the arrested fraction expresses HOC genes at low levels, the *fractional* increase in the levels of those genes would be much larger in HOC phase as is observed in the data, Figure 3.

7 Periodic Expression of Genes Annotated to the CDC in Non-dividing Cells

One could conceive that the genes annotated to the CDC are expressed periodically in the small subset of cells that divided. In addition to the arguments presented in the main paper, a few observations make this possibility very unlikely. First, if those genes were expressed only in the dividing cells, they should be expressed at higher levels in the glucose reference ($\mu = 0.25h^{-1}$) in which more than 60% of the cells are budded and the population doubling time is 2.8 hours (4). In contrast, we observed that about half of the periodic genes are expressed more highly in our batch culture compared to the reference, Figure 4 left set of panels. The second observation is that the genes are cycling with steady amplitudes, in synchrony with the oxygen oscillations, although the fraction of cells with duplicated DNA decreases *monotonically* by an order of magnitude, Figure 2C and 2D. Thus, the genes from the second cluster were expressed in the cells that cycled metabolically cells rather than in the cells that divided.

8 Number of mRNAs per Cell

As noted in the discussion, a possible reason for the periodic expression of most mRNAs (Figure 3) is that such a periodic mode of regulation is better suited to the regime of very low copy number molecules. Indeed, we found such evidence for very low copy number in slowly growing yeast cells. We studied 18 mRNAs selected to be expressed periodically with the YMC and to change expression levels with changes in the growth rate (8). We used fluorescent *in situ* hybridization (FISH) to count single mRNAs in singe cells and found that for any coexpressed pair of genes most cells do not have even a single mRNA molecule while some cells have $20 - 40$ molecules from both. Most of the 18 mRNAs are expressed at only $1 - 2$ or fewer molecules per cell on average in glucose limited cultures grown at growth rate $\mu = 0.10h^{-1}$, Figure S6. The number of mRNA molecules counted by FISH might underestimate the actual number on mRNAs per cell as some mRNAs may be inaccessible to the probes (because they are bound by protein complexes for example) but it is among the best available empirical estimates.

We sought to test the generality of this observation by extrapolating the results for those 18 genes to the whole genome. First we found a linear correspondence between the expression levels of those 18 genes measured by Affymetrix array in glucose limited cultures grown at the same growth rate $\mu = 0.10h^{-1}$, Figure S6B. Then we

used the inferred linear proportionality to convert the levels of all other genes measured on the Affymetrix array into average number of mRNAs per cell, Figure S6CD. As extrapolation, the results should be interpreted with caution but if they are anywhere close to the reality, slowly growing cells express most genes at very low levels, below 1 molecule per cell on average, Figure S6CD. If the expression of such lowly expressed genes is gradual (analog like tuning of the probability of the their transcription), the signal to noise ratio (SNR) is going to be very low because of inevitable counting noise. In contrast, expressing such genes at relatively high levels ($20-40$ per cells) during short periods when they are needed and not at all during the rest of the time can afford more reliable regulatory mechanism. This mode of expression consisting of temporally organized discrete bursts may be particularly useful for slowly growing cells and not essential for fast growing cells (fermenting in rich media) and for constitutively expressed genes, (9).

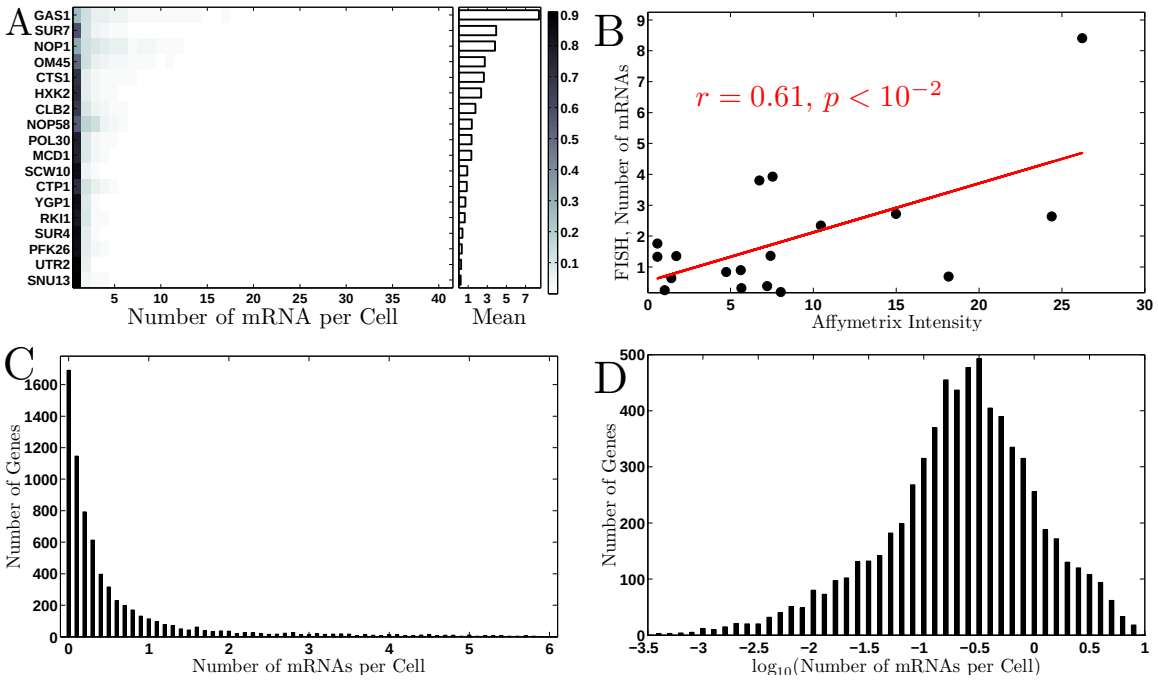

Figure S6. Number of mRNAs per Cell (A) Distribution and mean number of mRNAs in glucose limited cultures ($\mu = 0.1h^{-1}$) for 18 genes counted by single mRNA fluorescent *in situ* hybridizations (8). (B) Correlation between the the mean number of those 18 mRNAs and their mean expression as measured by Affymetrix micro-arrays (7). (C) Distribution of mRNAs per cell for each genes in the genome calculated from the linear fit on panel (B) and the Affymetrix data for all genes. (D) Distribution of the $\log_{10}$ transformed data from panel (C).

References

1. Slavov N, Botstein D (2011) Coupling among growth rate response, metabolic cycle, and cell division cycle in yeast. *Mol. Biol. Cell* 22:1997–2009.

2. Saldanha AJ, Brauer MJ, Botstein D (2004) Nutritional homeostasis in batch and Steady-State culture of yeast. *Mol. Biol. Cell* 15:4089–4104.

3. Brauer MJ, Saldanha AJ, Dolinski K, Botstein D (2005) Homeostatic adjustment and metabolic remodeling in glucose-limited yeast cultures. *Molecular Biology of the Cell* 16:2503–2517 PMID: 15758028 PMCID: 1087253.

4. Brauer MJ, et al. (2008) Coordination of growth rate, cell cycle, stress response, and metabolic activity in yeast. *Mol. Biol. Cell* 19:352–367.

5. Ronen M, Botstein D (2006) Transcriptional response of steady-state yeast cultures to transient perturbations in carbon source. *Proceedings of the National Academy of Sciences of the United States of America* 103:389–394.

6. Cai L, Sutter BM, Li B, Tu BP (2011) Acetyl-CoA induces cell growth and proliferation by promoting the acetylation of histones at growth genes. *Molecular Cell* 42:426–437.

7. Tu BP, Kudlicki A, Rowicka M, McKnight SL (2005) Logic of the yeast metabolic cycle: Temporal compartmentalization of cellular processes. *Science* 310:1152–1158.

8. Silverman SJ, et al. (2010) Metabolic cycling in single yeast cells from unsynchronized steady-state populations limited on glucose or phosphate. *Proceedings of the National Academy of Sciences*.

9. Zenklusen D, Larson DR, Singer RH (2008) Single-RNA counting reveals alternative modes of gene expression in yeast. *Nat Struct Mol Biol* 15:1263–1271.